Available online at www.sciencedirect.com

SciVerse ScienceDirect

Ceramics International 38 (2012) 6629–6634

CERAMICS INTERNATIONAL

www.elsevier.com/locate/ceramint

High-temperature resistant glass-ceramics based on Sr-anorthite and tialite phases

L.A. Orlova[a], N.V. Popovich[a], N.E. Uvarova[a], A. Paleari[a,b,*], P.D. Sarkisov[a]

[a]International Laboratory of Glass-based Functional Materials, Mendeleev University of Chemical Technology of Russia, Miusskaya Square 9, 125190 Moscow, Russia

[b]Department of Materials Science, University of Milano-Bicocca, Via R. Cozzi 53, I-20125 Milano, Italy

Received 27 January 2012; received in revised form 8 May 2012; accepted 16 May 2012
Available online 23 May 2012

Abstract

We have identified a convenient strategy for the control of the thermal growth of monoclinic Sr-anorthite and tialite phases in Sr–Ti–Al–silicates. The proposed method gives rise to a novel glassceramic material with thermal, mechanical, and dielectric properties potentially interesting in applications which require high temperature resistant radiotransparent materials. Crucially, we have found that the selective growth of Al_2TiO_5 and monoclinic $SrAl_2Si_2O_8$ is enabled by keeping the SrO/Al_2O_3 ratio lower than unity. This strategy permits to prevent the crystallisation of detrimental rutile and hexagonal Sr-anorthite. Interestingly, the stable properties of monoclinic Sr-anorthite, never used in conjunction with tialite, give rise to a glassceramic system with good mechanical resistance (micro-hardness 9.6 GPa, modulus of rupture 100 MPa) and with relatively stable values of thermal expansion (49×10^{-7} °C^{-1} from 20 to 1250 °C), thermal diffusivity (0.45×10^{-6} m^2 s^{-1}), thermal conductivity (1.0 W °C^{-1} m^{-1}), and dielectric constant (8.2) up to 1200 °C.

Keywords: C. Thermal properties; C. Mechanical properties; D. Glass ceramics; E. Refractories

1. Introduction

The development of heat-power engineering, as well as aircraft- and space-technology, calls for new materials with good mechanical properties and improved resistance to high temperature (HT) conditions. Interesting results were obtained by joining the high thermal and mechanical hardness of alumino-silicate phases, such as anorthite ($CaAl_2Si_2O_8$) and mullite ($Al_6Si_2O_{13}$), with Zr or Ti oxides [1–5]. However, the increasing innovation asks for new ceramics and glass-ceramics with extended working temperature range. For this reason several studies are currently devoted to composite systems, composed of ceramics and metal alloys, fibres, and other compounds [6–10]. In this regard, the use of glassy matrices to embed nano- or micro-phases with specific structural or functional properties in a easily workable material is becoming more and more strategic in several technological areas [11]. Particularly in the field of HT materials, the need of high working temperature is often accompanied by other stringent requirements. Crucially, as regards aircraft industry, the demand of HT materials – with a thermal expansion low enough to prevent structural deformation – has to be conjugated with reduced electrical conductivity and dielectric losses to avoid electromagnetic shielding and interference of radio-technical devices protected by HT barriers [12]. Some of the available industrial solutions for radio-transparent HT barriers – regarding oxide materials – are the result of two main strategies. One is based on solid solutions of cordierite ($2MgO–2Al_2O_3–5SiO_2$), rutile (TiO_2), and β-SiO_2 quartz (Pyroceram 9606, USA) [13], and the second one involves solid solutions of β-spodumene ($(Li_2O–Al_2O_3–4SiO_2$), TiO_2 and Al_2O_3 corundum (Pyroceram 9608) [14]. Some physical properties of these radio-transparent commercial glassceramics are summarized in Table 1 [13–16]. We note that the working temperature achievable without loss of the required features is lower than or at most equal to 1000 °C in these reference materials. Different

*Corresponding author at: Department of Materials Science, University of Milano-Bicocca, Via Cozzi 53, I-20125 Milano, Italy.
Tel.: +39 02 64485164; fax: +39 02 64485400.
E-mail address: alberto.paleari@mater.unimib.it (A. Paleari).

0272-8842/$36.00
http://dx.doi.org/10.1016/j.ceramint.2012.05.049

Table 1
Density (ρ), modulus of rupture (MoR), micro-hardness (μh), thermal expansion coefficient (α), maximum working temperature (T_w), softening point (T_s)) of commercial Pyroceram 9606 and 9608 [13–16], compared with sample C (this work).

	Pyr9606	Pyr9608	*C*
ρ (kg/m ^{3})	2610	2500	2990
MoR (MPa)	120–260	110–130	100
μh (MPa)	6845	6894	9600
α (10^{-7} K^{-1})	52[a]	20[b]	49[c]
T_w (°C)	800	900	1200
T_s (°C)	1350	1250	1400

[a]In the range 20–1000 °C.
[b]In the range 20–60 °C.
[c]In the range 20–1250 °C.

aluminates and silicates could in principle be considered, particularly among Ti- and Sr-oxides, typically characterized by high melting temperature.Tialite has indeed a well known potential as refractory materials [17]. Analogously, strontium compounds, specifically strontium aluminates, could also be interesting and are indeed used in several technological applications [18]. However, as concerns Sr-anorthite, there are only few studies on HT applications [19–21], notwithstanding the high melting point (1760 °C), low thermal expansion (3×10^{-6} K^{-1}), and suitable dielectric constant (6 at 10^{10}Hz).

Here we show that a net increase of the working temperature can be achieved, together with reduced thermal expansion and adequate dielectric features, starting from the SrO–TiO_2–Al_2O_3–SiO_2 system. The rationale of the present approach is, on the one hand, to take advantage of the good thermal and mechanical properties of monoclinic Sr-anorthite [22–24], and on the other hand to employ the peculiar propensity of strontium ion for keeping its coordination fixed in aluminium-silicates [23], so as to induce the parallel crystallisation of tialite (Al_2TiO_5) from an excess of aluminium oxide in the starting glass, and to avoid the separation of TiO_2. The results confirm that the formation of a solid solution of Sr-anorthite ($SrAl_2Si_2O_8$) and tialite can be driven from the crystallisation of SrO–TiO_2–Al_2O_3–SiO_2 glasses, by controlling the SrO/Al_2O_3 ratio. According to the proposed strategy, we have obtained a new glassceramic material with thermal, mechanical and dielectric properties that turn out to be potentially interesting in the technological areas of HT-resistant radio-transparent silicate ceramics, as well as in the field of coating and composites systems for HT thermal barriers.

2. Experimental procedure

SrO–TiO_2–Al_2O_3–SiO_2 glasses were prepared starting from powders of Si, Al, Ti oxides and Sr carbonate. Specifically, according to supplier certifications and GOST Russian standards, raw materials were SiO_2 quartz powder (99.0% pure, Fe_2O_3 less than 0.02%, Al_2O_3 less than 0.4%) with particle size in the range 0.1–0.4 mm (GOST 22551-77), α-Al_2O_3 alumina powder (purity higher than 94%, SiO_2 less than 0.1%, Fe_2O_3 less than 0.03%, Na_2O and K_2O less than 0.1%) with grain size 5 μm (90%, GOST 30559-98), $SrCO_3$ reagent (99.9% pure, according to GOST 2821-75), TiO_2 (98% pure, rutile phase higher than 97%) with particle size between 4.5 and 160 μm (GOST 9808-84 standard). The reagents were mixed in planetary agate mill for 5 min. The sample batch was then placed in corundum crucibles, without compaction, and was melted at 1600 °C for 10 h in gas-flame furnace under oxidizing conditions. All glasses were then annealed at 700 °C. The molar ratio of SrO to Al_2O_3 was kept either consistent with or deviating from the value expected in Sr-anorthite $SrAl_2Si_2O_8$. Specifically, samples with molar composition 14.2SrO–14.0TiO_2–14.8Al_2O_3–57.0SiO_2 and 16.8SrO–14.5TiO_2–17.1Al_2O_3–51.6SiO_2 were prepared starting from a SrO/Al_2O_3 molar ratio close to unity (*A* and *B* samples, respectively, in Fig. 1), while a sample with composition 15.1SrO–9.8TiO_2–23.0Al_2O_3–52.1SiO_2 (*C* sample in Fig. 1) was prepared with an excess of

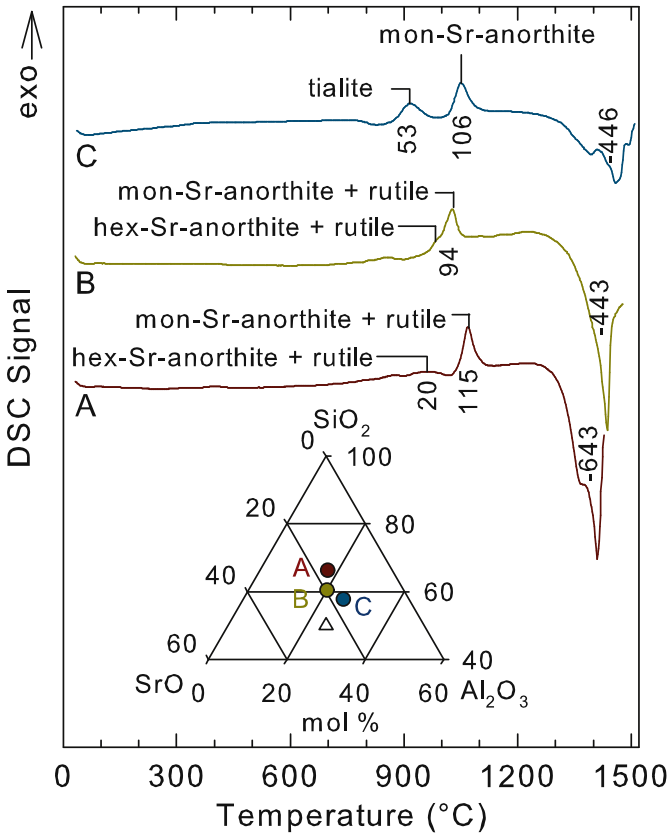

Fig. 1. Differential scanning calorimetry curves collected on three SrO–TiO_2–Al_2O_3–SiO_2 glasses (samples *A*, *B*, and *C*) with molar compositions indicated (except for TiO_2 content) in the triangular SrO–Al_2O_3–SiO_2 diagram in inset, together with the nominal composition of crystalline anorthite $SrAl_2Si_2O_8$ (open triangle). Crystallisation temperatures of hexagonal anorthite (hex-Sr-anorthite), monoclinic anorthite (mon-Sr-anorthite), rutile, and tialite phases (from XRD analysis) are evidenced. Integrated values of the peaks in J/g are also indicated.

Al_2O_3 amount with respect to the anorthite stoichiometry. The fraction of SiO_2 in the investigated samples was larger than 50 mol% so as to assure the formation of a silicate matrix as a host of the crystalline phase. The amount of TiO_2 – added in excess to the Sr–Al–Si compositions as crystallisation agent – was kept in the range 10–14 mol%.

Crystallisation and glassceramic formations were analysed through differential scanning calorimetry (DSC) and x-ray diffraction (XRD) analysis of fine powders (sieve 0.063 mm) of the obtained glasses. DSC measurements were performed by means of a high-temperature Netzsch STA 449C Jupiter thermal analyser, heating the samples in corundum crucibles at constant heating rate of 10 °C/min between 20 °C and 1550 °C in air, with an empty crucible as a reference standard. The thermally induced crystalline phases were identified ex situ through XRD analysis of samples subjected to isochronal annealing procedure between 750 and 1350 °C in successive 1 h heating steps of 100 °C. XRD measurements were collected by means of a DRON-3M diffractometer, using CuKα radiation over a scanning range $2\theta = 10-60°$. Identification of phases was based on the electronic catalog JCDFS. The intermediate samples were also analysed by means of electron scanning microscopy (JEOL JSM-6480LV and Quanta 3D FEG) to control the effects of the crystallisation on the microstructure.

The density of the materials was determined by the Archimedes method. For mechanical tests (Modulus of Rupture (MoR) and microhardness) bars of appropriate size were cut from the samples. MoR values were determined by means of a tensile testing machine T1-FRO10THW/A50 Zwick, with an uncertainty of 10 MPa. The linear thermal expansion coefficient from room temperature to 1400 °C was measured in air on bar specimens with 25 mm length by using a high-temperature dilatometer (Model DIL 402 PC, Netzsch). The data were recorded at heating rate of 5 °C/min. Thermal diffusivity was evaluated from 20 to 1300 °C by means of a TS-3000 H/L device using the laser pulse method. Thermal conductivity measurements were carried out by measuring the temperature on the opposite faces of the samples in stationary heat flow conditions. Dielectric constant and dielectric loss were determined at the frequency of 10^{10} Hz by means of an Agilent Technologies N5230C device.

3. Results and discussion

In Fig. 1 we reports DSC curves of samples A, B, and C. The data show the formation of crystalline phases from approximately 850 °C up to the main exothermic peak at 1030–1070 °C. Importantly, the endothermic features ascribable to starting softening of the residual glass and possible crystals re-dissolution are found only at temperature higher than 1350 °C. XRD data on samples extracted at various steps of the heat treatment show that the main exothermic peak above 1000 °C – observed in all the investigated compositions – corresponds to the formation of monoclinic Sr-anorthite. Other exothermic peaks are however detected, with relevant differences by changing the starting glass composition. In particular, the exothermic contributions in the 960–1000 °C range in samples *A* and *B* are related to the formation of hexagonal anorthite and TiO_2. By contrast, the main crystallisation peak in sample *C* is caused by the growth of monoclinic Sr-anorthite and it is only accompanied by Al_2TiO_5 crystallisation at 918 °C.

Interestingly, the comparison of the DSC curves indicates that glass compositions with SrO/Al_2O_3 ratio close to unity enable the crystallisation of the high resistant Sr-variant of the anorthite monoclinic phase. However, the same data point out that hexagonal anorthite may grow as well, in some cases, together with different types of Ti-containing crystalline phases arising from the amount of titanium dioxide introduced as crystallising agent. It is to be noted that the formation of hexagonal anorthite is detrimental to the thermo-mechanical properties of the resulting material, since it undergoes to a phase transformation above room temperature [25] which usually leads to the occurrence of micro-cracks during heating and cooling processes. Importantly, we observe the formation of hexagonal anorthite in strict correlation with the detection of TiO_2 segregation, whereas no trace of TiO_2 – nor hexagonal anorthite – is found in samples prepared from a starting glass composition in which we have included an excess of Al content with respect to the anorthite SrO/Al_2O_3 ratio. This result indeed demonstrates the strong propensity of strontium to coordinate with a congruent number of Al and Si sites in the shell of next neighbours in aluminium silicates, similarly to what observed also during phase transformations [22]. In this situation, at SrO/Al_2O_3 close to unity, almost all Al sites turn out to participate to the crystallisation of Sr-anorthite, which thus hinders the reaction of the added amount of TiO_2 with Al_2O_3 to form the tialite Al_2TiO_5 phase. By contrast, the Al_2O_3 excess in *C*-glass enables the formation of the tialite Al_2TiO_5 phase instead of rutile. Crucially, tialite possesses good properties of low thermal expansion (2×10^{-6} K^{-1} at about 1000 °C) but it usually undergoes to eutectoid decomposition in its parent oxides, alumina and rutile, in the temperature range 750–1280 °C. The decomposition rate is however strongly dependent on the presence of other oxides (such as Fe_2O_3, MgO, SiO_2, ZrO_2, ZrSiO4, La_2O_3) which can form solid solutions with the aluminum titanate. These oxides, depending on their concentration, can make the material stable on a time scale of hundreds hours at the temperature of the maximum decomposition rate (1000–1100 °C). Therefore, as in other glassceramics in which tialite is combined with silicate phases [2,26], the problem of the low mechanical strength of tialite is expected to be removed in solid solution with Sr-anorthite, as indeed confirmed in sample *C* (Table 1). In order to optimize the design of the fabrication process, samples from composition *C* were further analysed as a function of the thermal treatment.

The thermal expansion coefficient α of the composition *C* is shown in Fig. 2 as a function of the heat treatment temperature. The data show that α becomes quite low after treatment above 1000 °C. This temperature just corresponds to the end of the crystallisation process, as evidenced by the exothermic peak (Fig. 1) and also by the drastic increase of XRD intensity of the tialite and monoclinic Sr-anorthite phases (inset in Fig. 2). Furthermore, heat treatments at increasing temperature along the DSC curves cause a relevant shift of both the transition glass temperature T_g and the deformation temperature T_d (Fig. 2). Interestingly, the thermal expansion coefficient does not show relevant changes at around 1200 °C (Fig. 2), that is a promising precondition for structural stability at that temperature. A good stability, at least on the time scale of hours, is indeed confirmed by XRD data (inset of Fig. 2), which do not register any indication of tialite phase decomposition throughout all the isochronal annealing experiments. In fact, in these experiments, samples were annealed in successive heating steps of 1 h at fixed temperature in the range 750–1350 °C, without any evidence of decomposition even after repeated treatments.

The microstructure in this sample after different heat treatments is reported in Fig. 3, showing a corrugation that starts at the beginning of the temperature range of crystallisation. Importantly, the size of the microstructure features appearing at the onset of the crystallisation process does not significantly change by increasing the treatment temperature. In fact, as one can see by comparing samples

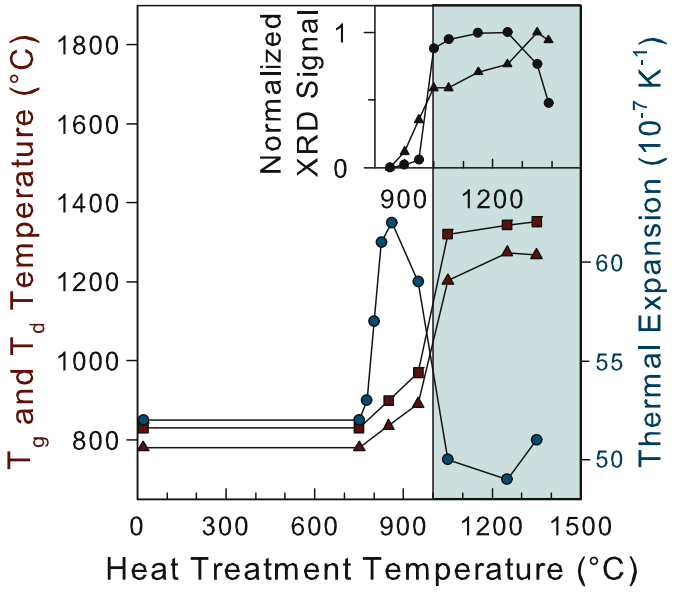

Fig. 2. Thermal expansion coefficient (circles, right axis), glass transition temperature T_g (triangles, left axis), and deformation temperature T_d (squares, left axis) in 15.1SrO–9.8TiO_2–23.0Al_2O_3–52.1SiO_2 material (sample *C*) treated at different temperatures. Inset: intensity of the XRD pattern (normalized to the maximum value) of monoclinic Sr-anorthite (circles) and tialite (triangles). The dashed area indicates the suitable treatment temperature range for the production of Sr-anorthite–tialite glassceramics.

treated at 1050 °C and at 1250 °C, the microstructure keeps an average size of the order of few μm, up to the completion of the crystallisation process. No fracture or cracks are observed after treatment at the main crystallisation exothermic peak at 1050 °C, reflecting the good structural stability of the material.

The formation of a solid solution of Sr-anorthite and tialite in the silicate matrix has indeed induced interesting properties as concerns the HT utilization as radio-transparent heat barrier. In fact, we observe reduced temperature dependences of the main thermal and dielectric properties. Fig. 4 summarizes the data of specific heat capacity (Fig. 4(a)), thermal diffusivity (Fig. 4(b)), and thermal conductivity (Fig. 4(c)) of the 15.1SrO–9.8TiO_2–23.0Al_2O_3–52.1SiO_2 composition in the range 20–1200 °C, compared with data of reference commercial materials (from Table 1 and quoted references). We note that the results on Sr-anorthite–tialite glassceramics show comparable percentage variations but in a wider temperature range and, importantly, with smaller values. As a matter of fact, the new glassceramics appears particularly interesting for the low and weakly temperature dependent values of thermal diffusivity and thermal conductivity, the latter one changing by only a factor 0.15 from room temperature to 1200 °C.

Fig. 5 shows the data of relative dielectric function ϵ_r and dielectric loss $tg(\delta)$. These data evidence a reduced temperature dependence of the dielectric response. In fact, ϵ_r increases by only 2% from room temperature to 1200 °C, largely less than in reference materials. The increase of $tg(\delta)$ is instead apparently large, particularly in the high temperature range above 800 °C. No data is available on commercial materials above 500 °C for a direct comparison. However, taking as a reference the variation of ϵ_r from 20 to 500 °C in commercial materials, we note that Sr-anorthite tialite glassceramics changes by the same factor in a wider temperature range, from 20 to 800 °C. Actually, even though the temperature dependence is weak, both ϵ_r and $tg(\delta)$ show higher values in the whole temperature range with respect to spodumene- or cordierite-based commercial materials. Nevertheless, their values are comparable or lower than in other radio-transparent ceramics based on silicon nitride compounds [27]. Taking into account all these evaluations, the mechanical, thermal, and dielectric properties of Sr-anorthite and tialite silicate glassceramics produced with the proposed strategy appear to be suitable for relatively high temperature applications.

4. Conclusion

In summary, we have verified the possibility to obtain novel glassceramic materials based on the use of monoclinic Sr-anorthite grown in titanium alumino-silicate glass. We have found that the crystallisation of anorthite and tialite can be controlled through the SrO/Al_2O_3 ratio so as to avoid the segregation of rutile and the formation of hexagonal anorthite. The resulting mechanical, thermal,

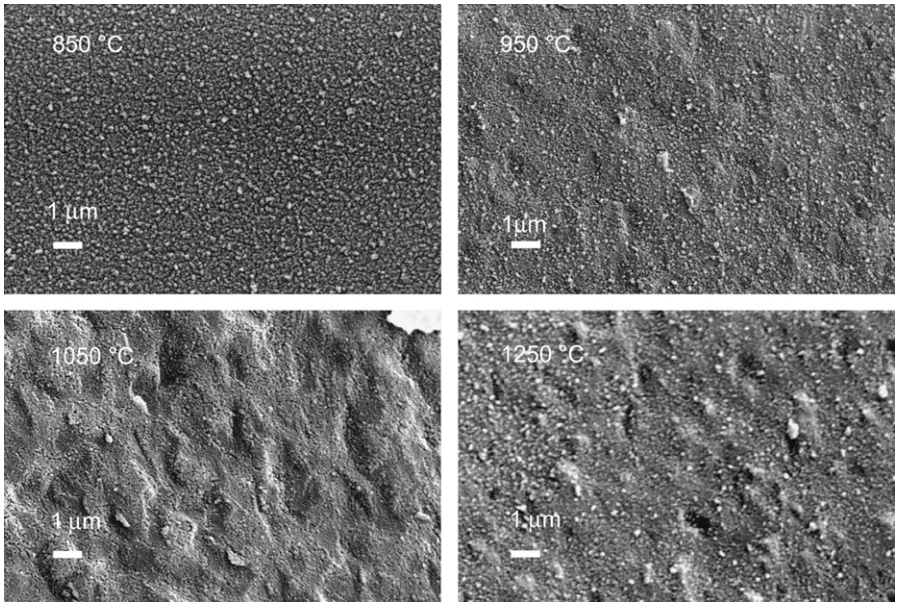

Fig. 3. SEM images of the microstructure of 15.1SrO–9.8TiO_2–23.0Al_2O_3–52.1SiO_2 material (sample *C*) treated at the indicated temperatures.

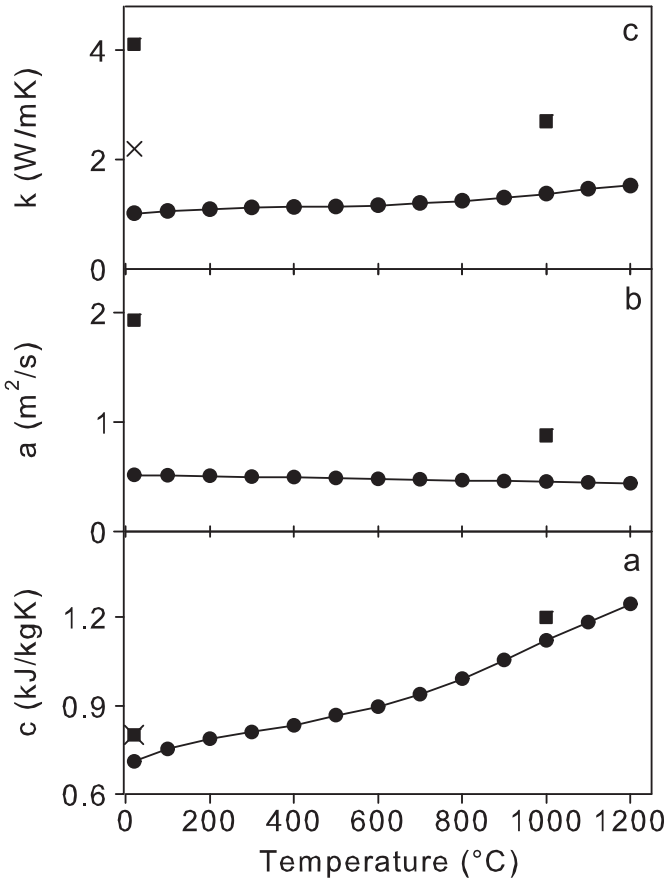

Fig. 4. Temperature dependence of (a) specific heat capacity, (b) thermal diffusivity, (c) thermal conductivity of 15.1SrO–9.8TiO_2–23.0Al_2O_3–52.1SiO_2 material (composition *C*) (circles). Values of pyroceram 9606 and 9608 reference materials (squares and crosses, respectively) are also reported.

and dielectric properties are promising for HT applications as radio-transparent materials in an extended range of temperature.

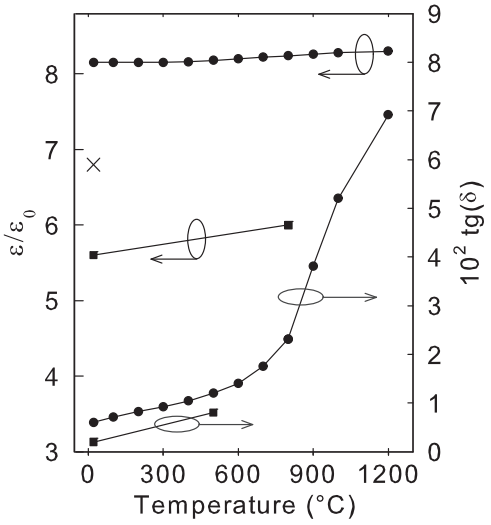

Fig. 5. Temperature dependence of the relative dielectric constant ϵ_r (ϵ/ϵ_0, left axis) at 10^{10} Hz and the dielectric loss $tg(\delta)$ (right axis) of 15.1SrO–9.8TiO_2–23.0Al_2O_3–52.1SiO_2 (composition *C*) (circles), compared with data of pyroceram 9606 (squares) and dielectric constant of pyroceram 9608 cross.

Acknowledgements

The authors gratefully acknowledge the financial support by the Ministry of Education and Science of Russia Federation under Grant No. 11.G34.31.0027.

References

[1] B.G. Nair, Q. Zhao, R.F. Cooper, Geopolymer matrices with improved hydrothermal corrosion resistance for high-temperature applications, Journal of Materials Science 42 (2007) 3083–3091.
[2] A. Tsetsekou, A comparison study of tialite ceramics doped with various oxide materials and tialite-mullite composites: microstructural, thermal and mechanical properties, Journal of the European Ceramic Society 25 (2005) 335–348.

[3] M. Takahashi, M. Fukuda, M. Fukuda, H. Fukuda, T. Yoko, Preparation, structure, and properties of thermally and mechanically improved aluminum titanate ceramics doped with alkali feldspar, Journal of the American Ceramic Society 85 (2002) 3025–3030.
[4] S. Kurama, E. Ozel, The influence of different CaO source in the production of anorthite ceramics, Ceramics International 35 (2009) 827–830.
[5] I.M. Low, C.G. Shi, Physical and thermal characteristics of aluminium titanate dispersed with β-spodumene and zirconia, Journal of Materials Science 35 (2000) 6293–6300.
[6] N.P. Padture, M. Gell, E.H. Jordan, Thermal barrier coatings for gas-turbine engine applications, Science 296 (2002) 280–284.
[7] A. Aygun, A.L. Vasiliev, N.P. Padture, X. Ma, Novel thermal barrier coatings that are resistant to high-temperature attack by glassy deposits, Acta Materialia 55 (2007) 6734–6745.
[8] R. Bermejo, A.J. Sánchez-Herencia, L. Llanes, C. Baudín, High-temperature mechanical behaviour of flaw tolerant alumina-zirconia multilayered ceramics, Acta Materialia 55 (2007) 4891–4901.
[9] A. Feuerstein, J. Knapp, T. Taylor, A. Ashary, A. Bolcavage, N. Hitchman, Technical and economical aspects of current thermal barrier coating systems for gas turbine engines by thermal spray and EBPVD: a review, Journal of Thermal Spray Technology 17 (2008) 199–213.
[10] M. Jayasankar, K.P. Hima, S. Ananthakumar, P. Mukundan, P. Krishna Pillai, K.G.K. Warrier, Role of particle size of alumina on the formation of aluminium titanate as well as on sintering and microstructure development in sol-gel alumina-aluminium titanate composites, Materials Chemistry and Physics 124 (2010) 92–96.
[11] E. Axinte, Glasses as engineering materials: a review, Materials & Design 32 (2011) 1717–1732.
[12] E.I. Suzdal'tsev, Fabrication of high-density quartz ceramics: research and practical aspects. Part 6. A comprehensive study of the properties of BN-modified densely sintered ceramics, Refractories and Industrial Ceramics 47 (2006) 101–109.
[13] D.R. Salmon, R. Brandt, R.P. Tye, Pyroceram 9606, a certified ceramic reference material for high-temperature thermal transport properties: part 2 – certification measurements, International Journal of Thermophysics 31 (2010) 355–373.
[14] E.I. Suzdal'tsev, D.V. Kharitonov, A.A. Anashkina, Analysis of existing radiotransparent refractory materials, composites and technology for creating high-speed rocket radomes. Part 3. Manufacturing technology for glass ceramic radomes problems and future improvement, Refractories and Industrial Ceramics 51 (2010) 289–294.
[15] S.D. Stookey, Catalyzed crystallization of glass in theory and practice, Industrial & Engineering Chemistry 51 (1959) 805–808.
[16] Z. Strnad, Glass-Ceramic Materials, Elsevier, New York, 1986.
[17] M. Nagano, S. Nagashima, H. Maeda, A. Kato, Sintering behavior of Al_2TiO_5 based ceramics and their thermal properties, Ceramics International 25 (1999) 681–687.
[18] R. Salda na Garcés, J. Torres Torres, A. Flores Valdés, Synthesis of $SrAl_2O_4$ and $Sr_3Al_2O_6$ at high temperature, starting from mechanically activated $SrCO_3$ and Al_2O_3 in blends of 3:1 molar ratio, Ceramics International 38 (2012) 889–894.
[19] N.P. Bansal, Mechanical behavior of silicon carbide fiber-reinforced strontium aluminosilicate glass-ceramic composites, Materials Science and Engineering: A 231 (1997) 117–127.
[20] R.E. Chinn, M.J. Haun, C.Y. Kim, D.B. Price, Low-temperature transient glass-phase processing of monoclinic $SrAl_2Si_2O_8$, Journal of the American Ceramic Society 81 (1998) 2285–2293.
[21] R.E. Chinn, M.J. Haun, C.Y. Kim, D.B. Price, Microstructure and properties of three composites of alumina,mullite, and monoclinic $SrAl_2Si_2O_8$, Journal of the American Ceramic Society 83 (2000) 2668–2672.
[22] P.A. Arifov, M.M. Bulatova, Triangulation and specific features of the phase formation in strontium aluminosilicate glass-forming systems, Glass Physics and Chemistry 30 (2004) 198–201.
[23] J.B. Parise, D.R. Corbin, M.A. Subramanian, The role of strontium in the densification of Sr-zeolite-A to the low dielectric ceramic, anorthite, Materials Research Bulletin 24 (1989) 303–310.
[24] A. Liebscher, M. Thiele, G. Franz, G. Doersam, M. Gottschalk, Synthetic Sr–Ca margarite, anorthite and slawsonite solid solutions and solid–fluid Sr–Ca fractionation, European Journal of Mineral 21 (2009) 275–292.
[25] S.A.T. Redfern, E. Salje, Microscopic dynamic and macroscopic thermodynamic character of the $I1-P1$ phase transition in anorthite, Physics and Chemistry of Minerals 18 (1992) 526–533.
[26] U.S. Hareesh, A.K. Vasudevan, P. Mukundan, A.D. Damodaran, K.G.K. Warrier, Low temperature sintering of seeded aluminium titanate precursor gels, Materials Letters 32 (1997) 203–208.
[27] F. Chen, Q. Shen, L. Zhang, Electromagnetic optimal design and preparation of broadband ceramic radome material with graded porous structure, Progress in Electromagnetics Research 105 (2010) 445–461.